

Communication

Turbo Equalization of 2-D Intersymbol Interference Using Multiple 1-D Constituent Equalizers

Jaehyeong No and Jaekyun Moon, *Fellow, IEEE*

Department of Electrical Engineering, Korea Advanced Institute of Science and Technology, Daejeon 305-701, Korea

A 2-D soft-in, soft-out equalizer consisting of multiple low-complexity constituent equalizers is proposed for the turbo equalization of 2-D intersymbol interference. The constituent equalizers are simple 1-D linear equalizers running in different directions over a 2-D array of storage cells. Simulation results as well as an extrinsic information transfer chart analysis indicate that the proposed concatenation provides performance comparable with finite-window trellis-based equalizers while requiring a much lower complexity level.

Index Terms—2-D equalization, extrinsic information transfer (EXIT) chart, intersymbol interference (ISI), self-iterating soft equalizer.

I. INTRODUCTION

TWO-DIMENSIONAL intersymbol interference (2-D ISI) presents serious issues in the reliable data recovery of advanced high-density disk drive channels [1], [2] and flash memory devices [3]. 2-D ISI arises largely due to 2-D memory cells getting physically closer to one another with increasing storage density. In magnetic storage, 2-D ISI arises as the read resolution cannot keep up with the decreasing size of the magnetic cells [1], [2], while in the flash memory, 2-D ISI is mainly due to coupling of floating gate voltages in neighboring cells [3]. With 2-D ISI, presenting an increasingly significant issue, efficient 2-D signal processing becomes critical in reliable data recovery. In particular, 2-D ISI equalization is expected to play a key role along with powerful error-correcting codes.

In 2-D environments, equalization complexity grows even more quickly with increasing ISI compared with the 1-D situation as the ISI comes from multiple radial directions. Accordingly, keeping the complexity level low without sacrificing performance significantly is an important objective in the 2-D equalizer design. To this end, we consider turbo equalization using a low-complexity 2-D equalization scheme based on multiple self-iterating soft linear equalizers running in three different directions over a 2-D array of cells. The basic idea behind the multidirectional self-iterating soft equalizer (MD-SISE), first discussed in [4], is to concatenate multiple 1-D SISO linear equalizers that are simple but, when working together, would produce reliable decisions. The idea of constructing a strong self-iterating equalizer based on multiple, relatively weak equalizers has been suggested for severe 1-D ISI channels in [5].

In this paper, we discuss the application of MD-SISE to 2-D turbo equalization setting; we, in particular, devise a simple way of incorporating the effect of hard-decision cancellation of offtrack interference in the extrinsic information transfer (EXIT) chart analysis and also establish a method

Manuscript received November 10, 2014; revised January 7, 2015; accepted May 3, 2015. Date of publication May 12, 2015; date of current version August 17, 2015. Corresponding author: J. Moon (e-mail: jmoon@kaist.edu).

Color versions of one or more of the figures in this paper are available online at <http://ieeexplore.ieee.org>.

Digital Object Identifier 10.1109/TMAG.2015.2431991

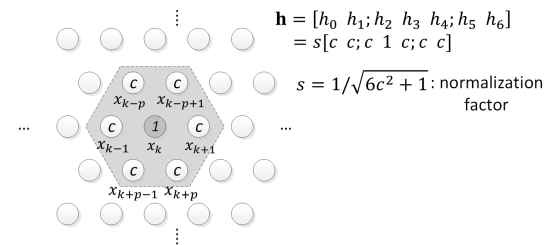


Fig. 1. 2-D array of data symbols, the ISI mask and the channel matrix.

to understand the iterative interactions of the constituent equalizers [e.g., to estimate the number of self-iterations (SIs) required to reach full performance potential of the MD-SISE].

There have been various works on 2-D equalization based on the maximum *a posteriori* (MAP) probability scheme [6], [7]. Unfortunately, it is known that 2-D MAP-based sequence detection is in general NP hard [8]. The concept of combined multiple equalizers running in different directions has also been considered in [7], but the constituent equalizers based on reduced-state trellis processing require significant complexity in 2-D ISI environments. In this paper, we put great emphasis on low complexity and demonstrate that using only simple linear constituent equalizers, we can achieve turbo equalization performance comparable with that obtained using much more complex finite-state MAP-based equalization schemes.

II. CHANNEL ASSUMPTIONS

Consider a 2-D array of data symbols with an ISI mask, as shown in Fig. 1. The small circular islands represent bit cells where the data is stored. The ISI mask is assumed to be of a hexagonal shape in this paper. In the read process, as the ISI mask scans over the data cells, the read signal corresponding to a given position of the mask is simply a linear combination of the stored values for the cells captured under the mask. For the particular ISI mask shown in the figure, there are six interfering edge cells affecting the center cell. The amount of interference is simply characterized by the single parameter c that controls the weights on the interference. We rewrite the 2-D channel response matrix \mathbf{h} into a 1-D channel vector $\mathbf{h} = [h_0 \dots h_6]^T$

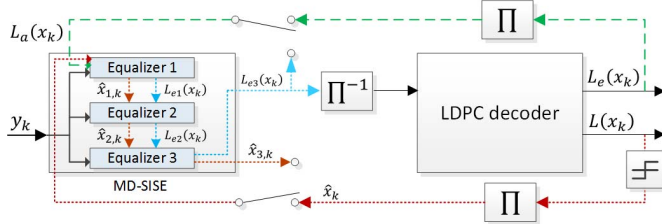


Fig. 2. MD-SISE based turbo equalizer.

for direct application of known equalization methods. Accordingly, the channel output is expressed as $y_k = \mathbf{x}_k^T \mathbf{h} + n_k$, where $\mathbf{x}_k^T = [x_{k-p} \dots x_k \dots x_{k+p}]$ and n_k is the sample of zero-mean Gaussian random noise. We assume that the time-invariant channel response weights in \mathbf{h} are known by the equalizer. The signal-to-noise ratio (SNR) is defined as the total signal power captured within the ISI mask, which is normalized to 1, divided by the noise variance σ_n^2 .

III. TURBO EQUALIZATION SETTING

Turbo equalization is a joint equalization and decoding scheme for coded data passed through a noisy channel also corrupted by ISI [9]. A SISO equalizer and a SISO decoder exchange extrinsic information in an iterative fashion until a desired performance level is achieved. The particular turbo equalization system under investigation is shown in Fig. 2. The MD-SISE consists of three constituent 1-D linear equalizers with each one generating soft decisions and passing them to another in the form of extrinsic information. Each constituent equalizer of the MD-SISE works in one of three directions: 1) horizontal; 2) diagonal; and 3) reverse diagonal, and passes extrinsic log-likelihood ratio (LLR) L_e that becomes *a priori* LLR L_a for the next constituent equalizer. This process continues until decision quality no longer improves or enough overall iterations have taken place. One SI means that the signals have been processed through the third constituent equalizer. The MD-SISE can continue on a new round of SI as the third constituent equalizer passes its extrinsic information back to the first constituent equalizer. Each constituent equalizer also passes hard decisions to the next constituent equalizer for the cancellation of the offtrack interference terms. The hard decisions are formed by slicing the updated soft information $L(x_k) = L_a(x_k) + L_e(x_k)$.

The output from the last constituent equalizer after a number of SIs is passed to the decoder through a shuffling device. The error correction code used here is a low-density parity check (LDPC) code. The LDPC decoder passes its extrinsic information as well as hard decisions back to the first constituent equalizer through the interleavers. One global iteration (GI) means a round of information exchange between the MD-SISE and the decoder. The two parallel switches included in Fig. 2 move at the same time, providing connections for either SI or GI at a given time.

To take a closer look at the hard-decision cancellation process, consider the dark gray islands in Fig. 3 corresponding to the tap positions of the horizontal constituent equalizer. Given the rotational symmetry of the ISI pattern, other constituent equalizers work in exactly the same way. The offtrack interference (coming from the lighter gray cells above and below the dark gray islands) is first canceled via hard-decision

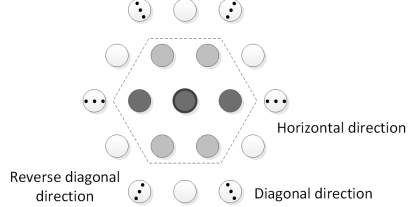


Fig. 3. Equalization directions for three constituent 1-D equalizers.

feedback $\hat{x}_{j,k}$ obtained from slicing $L(x_k)$, utilizing best up-to-date soft information in the collaborating constituent equalizer. Note that the passing of both $L_{e,j}$ and $\hat{x}_{j,k}$ occur in blocks, after each constituent equalizer completely scans the entire 2-D array of cells. Compared with the finite-state 2-D MAP-based equalizer, the MD-SISE suffers from a longer latency for scanning the entire 2-D array multiple times. This is the price paid for complexity reduction by orders of magnitude, as will be discussed shortly.

The updated observation after offtrack interference cancellation (IC) is given by $y'_k = y_k - \hat{\mathbf{x}}_k^T \mathbf{h}$ where $\hat{\mathbf{x}}_k^T = [\hat{x}_{k-p} \hat{x}_{k-p+1} 0 0 0 \hat{x}_{k+p-1} \hat{x}_{k+p}]$ for horizontal equalizing direction and the given ISI mask. Once offtrack IC is done, the minimum mean squared-error (MMSE) equalizer solutions are readily obtained in the form of the soft linear equalizer developed in [11]. To generate only the extrinsic information by suppressing the current symbol's *a priori* information, the equalizer output is expressed as

$$z_{e,j}(x_k) = \mathbf{g}_k^T (\mathbf{y}'_k - \mathbf{H}^T \bar{\mathbf{x}}_k + \bar{x}_k \mathbf{s}) \quad (1)$$

where \mathbf{g}_k is the vector of filter coefficients, \mathbf{y}'_k is the observation vector after offtrack IC, the overbar denotes the statistical mean (or a vector of means when placed over a vector), $\mathbf{s} = \mathbf{H}^T \mathbf{e}$, $\mathbf{e} = [0 \dots 0 1 0 \dots 0]^T$ with 1 placed at the k th position. The channel matrix \mathbf{H} is determined by the channel vector \mathbf{h} and zeros inserted for matching the dimensions between \mathbf{y}'_k and $\bar{\mathbf{x}}_k$. When we use a three-tap constituent equalizer for the given hexagonal ISI mask, the channel matrix is determined for horizontal equalizing direction as $\mathbf{H}^T = [h_2 \ h_3 \ h_4 \ 0 \ 0; \ 0 \ h_2 \ h_3 \ h_4 \ 0; \ 0 \ 0 \ h_2 \ h_3 \ h_4]$.

The time-varying equalizer tap weights and new L_e are given by

$$\mathbf{g}_k = \{\sigma_n^2 \mathbf{I}_N + \mathbf{H}^T \mathbf{R}_{xx,k} \mathbf{H} + (1 - v_k) \mathbf{s} \mathbf{s}^T\}^{-1} \mathbf{s} \quad (2)$$

$$L_{e,j}(x_k) = 2z_{e,j}(x_k)/(1 - \mathbf{s}^T \mathbf{g}_k) \quad (3)$$

where again σ_n^2 is the noise variance, \mathbf{I}_N is the identity matrix of size N , $\mathbf{R}_{xx,k}$ is the covariance matrix for the channel input, and v_k is the variance for each input symbol. The mean and the variance are calculated using the extrinsic LLR passed down from the previous constituent equalizer/decoder (which now has become the *a priori* LLR of the current constituent device): $\bar{x}_k = \tanh(L_a(x_k)/2)$ and $v_k = 1 - |\bar{x}_k|^2$, respectively. For the first SI on the first GI, the *a priori* probabilities for constituent equalizer 1 are all set to 1/2, and hard decisions for IC are determined by the simple threshold detection of the channel observations.

Since the performance losses associated with the quasi-time-invariant (QTI) filters (i.e., filter taps change only once for each constituent equalizer per SI) are only

marginal [4], [11] while complexity savings are considerable, we employ the following QTI taps:

$$\mathbf{g}_{\text{qti}} = (\sigma_n^2 \mathbf{I}_N + \mathbf{H}^T \bar{\mathbf{R}}_{xx} \mathbf{H})^{-1} \mathbf{s} \quad (4)$$

where $\bar{\mathbf{R}}_{xx}$ is the matrix replacing all variance terms in $\mathbf{R}_{xx,k}$ with a time-averaged version $\bar{v} = (1/D) \sum_{i=0}^{D-1} v_i$ (D is the data array size) except that v_k is forced to 1 (i.e., $\bar{\mathbf{R}}_{xx} = \text{diag}[\bar{v} \dots \bar{v} 1 \bar{v} \dots \bar{v}]$). Equations (1) and (3) are modified accordingly with \mathbf{g}_k replaced by \mathbf{g}_{qti} .

The direct 2-D MMSE equalizer that will be used for comparison is also based on (1) and (3) with the QTI filter utilized. The difference is that the dimension of \mathbf{H} in (1) is necessarily much larger with the direct 2-D MMSE equalizer than with the proposed MD-SISE, resulting in a substantial complexity burden. As for the Bahl–Cocke–Jelinek–Raviv (BCJR) equalizers [12], we force a finite-state machine by imposing a state mask, which controls performance/complexity tradeoff. More detailed descriptions of the direct 2-D MMSE equalizer and finite-state 2-D BCJR equalizers can be found in [4]. It is straightforward to put together turbo equalization systems using these constituent equalizers.

IV. PERFORMANCE ANALYSIS WITH EXIT CHART

Turbo equalization performance is often analyzed using the EXIT chart that provides useful insights about iterative systems without time-consuming simulation of the full signal-processing chain [13]. In the EXIT chart analysis, the output in the form of extrinsic information I_e is obtained for every value of the input *a priori* information I_a . However, in the proposed turbo equalization using the MD-SISE, a given constituent equalizer also utilizes the updated soft information L passed from the collaborating constituent equalizer (or the decoder in the case of GI). To handle this issue, we set out to find a reasonable way to generate hard decisions using only L_a or, equivalently, L_e passed from the previous constituent equalizer (or decoder). These decisions will be used to cancel offtrack interference during the simulation of the constituent equalizer for generating the histogram of its output or its extrinsic information that will be used for mutual information (MI) estimation.

It is well established that L_a can be modeled as an independent Gaussian random variable with a mean shift equal to half the variance, i.e., $L_a = \epsilon_a x / 2 + n(\epsilon_a)$, where $n(\epsilon_a)$ is Gaussian noise with zero mean and variance ϵ_a and $x \in \{+1, -1\}$ is the known data [13]. At the first SI with all zero L_a , suppose we can write $L = \epsilon_d x / 2 + n(\epsilon_d)$ where ϵ_d is such that $\epsilon_d = J^{-1}\{I(X; L)\}$. The function J here relates the given MI with the variance ϵ of the matching Gaussian probability density function [13]. Letting $I(X; Y)$ be the MI between the channel input and the unequalsized channel output, it is reasonable to write $I(X; L) \approx I(X; Y)$ when L_a are all zero. Thus, ϵ_d can be obtained from $\epsilon_d = J^{-1}\{I(X; Y)\}$ after estimating $I(X; Y)$ numerically using the histogram of Y . Now the combined variance $\epsilon_t = \epsilon_d + \epsilon_a$ is used for generating L with the fixed ϵ_d and ϵ_a that increases over iterations

$$L \triangleq \frac{\epsilon_t}{2} x + n(\epsilon_t). \quad (5)$$

Fig. 4 shows the extrinsic MI curves of the MD-SISE incorporating IC using the hard decisions made from L of (5).

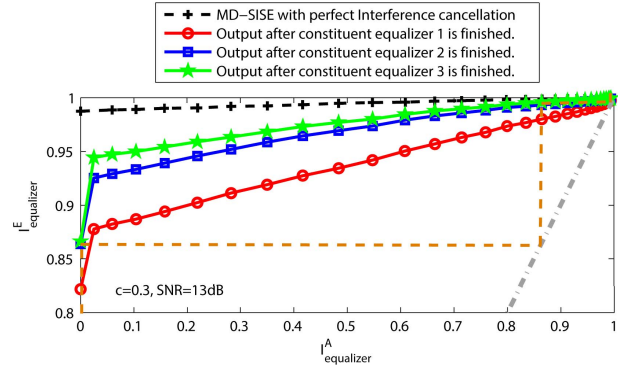


Fig. 4. Output versus input MI curves through SIs in MD-SISE.

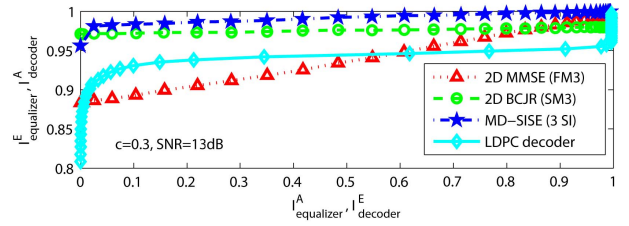


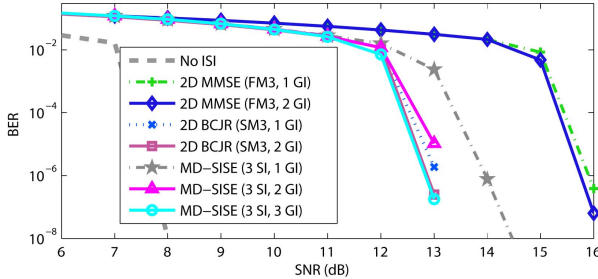
Fig. 5. EXIT chart for the different 2-D equalizers and the LDPC decoder.

The three I_E versus I_A curves represent the output MIs I_E at the outputs of the three constituent equalizers plotted versus I_A for constituent equalizer 1. There is a big jump in the extrinsic information quality going from constituent equalizer 1 to constituent equalizer 2 and then only a marginal improvement from constituent equalizer 2 to constituent equalizer 3. As ϵ_a increases and thus I_A improves, the quality of the extrinsic outputs becomes as good as that in the case of perfect hard decisions.

The input/output MI curve for the last constituent equalizer in Fig. 4 can also serve to extract information on how many SIs would be needed to reach full performance potential of the MD-SISE. First, draw a straight diagonal line connecting two corner points $(0, 0)$ and $(1, 1)$, which is shown as the dashed-dotted line in the figure. Then, this line and the MI curve for the third constituent equalizer form a tunnel through which an MI trajectory corresponding to SIs can be visualized. For example, at $I_A = 0$, one round of SI yields an I_E of ~ 0.865 at the output of the third constituent equalizer. In the second round of SI, I_A then becomes 0.865 and this eventually gives by the end of the second round an I_E close to one, as can be seen in the height of the second step in the figure. It is clear that with three steps overall, the full MI of one can be achieved. This indicates that no more than three SIs would be needed in fully realizing the potential of the MD-SISE for this 2-D ISI channel with $c = 0.3$ and $\text{SNR} = 13 \text{ dB}$.

Fig. 5 shows that for the given channel condition and decoder, the 2-D BCJR equalizer and the MD-SISE provide tunnel openings for the MI trajectories to move up through GIs, whereas the 2-D MMSE equalizer fails to make a tunnel opening. Although the 2-D BCJR equalizer is able to open up the tunnel, its width gets somewhat narrower with increasing I_A , relative to that for the MD-SISE.

The 2-D MMSE equalizer is based on a hexagonal filter mask FM3 that covers seven cells along a main axis (37 total filter taps), whereas the state mask SM3 for the

Fig. 6. BER performance of turbo equalization for $c = 0.3$.

BCJR equalizer gives rise to a trellis with 2^8 states, 2^5 input branches for each state, and three observation samples utilized for each branch metric computation [4]. The number of SIs is fixed to 3 for the MD-SISE. Note that while it is conceptually straightforward to use the 2-D BCJR or the 2-D MMSE equalizer as the constituent equalizers in our SISE setup, doing so has little merit in our case, since rotating the state/filter mask along different directions makes little or no changes in terms of the specific interfering cells utilized to generate the nominal signal values for the branch metric calculation. We also note that unlike in [7], our 2-D BCJR schemes do not utilize feedback decisions for cells outside the state mask, another reason why extra scans along additional directions do not collect significant independent information in our case.

V. SIMULATION RESULTS AND COMPLEXITY COMPARISON

The LDPC code is the array-based code of [10] with a codeword length of 8154 b, a code rate of 0.907, and a parity check matrix characterized by the column weight 5, the row weight 54, and the circulant matrix size of 139. The size of the 2-D bit array used in the simulation is 1024 b \times 1024 b. The number of LDPC decoder iterations is limited to 20. The min-sum algorithm is used for message passing. For each constituent equalizer, only three taps are allowed, since little is gained by taking more taps for the assumed ISI mask. We adopt the S-random interleaver with $S = 63$ [14].

Fig. 6 shows bit error rate (BER) performance of the turbo equalizers. The 2-D MMSE equalizers with FM3 perform the worst. There is little gain going from 1 GI to 2 GIs. The MD-SISE with 3 SIs and the 2-D BCJR equalizer with SM3 perform much better than the 2-D MMSE equalizer with FM3 and, compared with each other, give similar performance. In terms of the BER, the BCJR equalizer seems to have a slight edge in that 1 GI seems to give performance on par with or better than the MD-SISE with 2 GIs.

When considering complexity, the advantage of the MD-SISE is considerable over the BCJR equalizers. See Table I. The complexity level comparison in terms of the numbers of multiplications needed indicates a large relative advantage of orders of magnitude for the proposed MD-SISE.

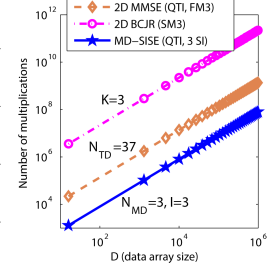
VI. CONCLUSION

In the turbo equalization setting for handling 2-D ISI, the proposed technique, which consists of multiple 1-D constituent equalizers working together via iterative exchange of soft information, can collaborate effectively with a SISO decoder to eventually reach highly reliable decisions. For hexagonal

TABLE I

REQUIRED COMPUTATIONS. $N_{TD} = (3N_C^2 + 1)/4$, THE NUMBER OF FILTER TAPS FOR 2-D MMSE. N_C , THE NUMBER OF TAPS ON A CENTER AXIS (e.g., $N_C = 7$ FOR FM3). N_{MD} , THE FILTER LENGTH FOR MD-SISE. K , THE NUMBER OF OBSERVATIONS ON A STATE MASK. I , THE NUMBER OF SI ROUNDS

scheme: number of multiplications
2D MMSE: $N_{TD}^2 D$
2D BCJR: $144KD \times 2^{3K}$
MD-SISE: $3N_{MD}^2 DI$



2-D ISI channels, it has been shown that the turbo equalizer using the proposed MD-SISE yields considerably better performance/complexity tradeoffs than that based on the direct 2-D MMSE equalizer or the finite-state 2-D BCJR equalizer.

ACKNOWLEDGMENT

This work was supported by the National Research Foundation of Korea under Grant 2010-0029205.

REFERENCES

- [1] T. Rausch *et al.*, "HAMR drive performance and integration challenges," *IEEE Trans. Magn.*, vol. 49, no. 2, pp. 730–733, Feb. 2013.
- [2] S. Nabavi, B. V. K. V. Kumar, and J. A. Bain, "Two-dimensional pulse response and media noise modeling for bit-patterned media," *IEEE Trans. Magn.*, vol. 44, no. 11, pp. 3789–3792, Nov. 2008.
- [3] J. Moon, J. No, S. Lee, S. Kim, S. Choi, and Y. Song, "Statistical characterization of noise and interference in NAND flash memory," *IEEE Trans. Circuits Syst. I, Reg. Papers*, vol. 60, no. 8, pp. 2153–2164, Aug. 2013.
- [4] J. No and J. Moon, "Multi-directional self-iterating soft equalization for 2D intersymbol interference," in *Proc. IEEE GLOBECOM*, Atlanta, GA, USA, Dec. 2013, pp. 2698–2704.
- [5] S. Jeong and J. Moon, "Self-iterating soft equalizer," *IEEE Trans. Commun.*, vol. 61, no. 9, pp. 3697–3709, Sep. 2013.
- [6] Y. Wu, J. A. O'Sullivan, N. Singla, and R. S. Indeck, "Iterative detection and decoding for separable two-dimensional intersymbol interference," *IEEE Trans. Magn.*, vol. 39, no. 4, pp. 2115–2120, Jul. 2003.
- [7] Y. Chen, P. Njeim, T. Cheng, B. J. Belzer, and K. Sivakumar, "Iterative soft decision feedback zig-zag equalizer for 2D intersymbol interference channels," *IEEE J. Sel. Areas Commun.*, vol. 28, no. 2, pp. 167–180, Feb. 2010.
- [8] E. Ordentlich and R. M. Roth, "Two-dimensional maximum-likelihood sequence detection is NP hard," *IEEE Trans. Inf. Theory*, vol. 57, no. 12, pp. 7661–7670, Dec. 2011.
- [9] C. Douillard, M. Jézéquel, C. Berrou, A. Picart, P. Didier, and A. Glavieux, "Iterative correction of intersymbol interference: Turbo-equalization," *Euro Trans. Telecommun.*, vol. 6, no. 5, pp. 507–511, Sep./Oct. 1995.
- [10] E. Eleftheriou and S. Olcer, "Low-density parity-check codes for digital subscriber lines," in *Proc. IEEE ICC*, Apr. 2002, pp. 1752–1757.
- [11] M. Tüchler, R. Koetter, and A. C. Singer, "Turbo equalization: Principles and new results," *IEEE Trans. Commun.*, vol. 50, no. 5, pp. 754–767, May 2002.
- [12] L. Bahl, J. Cocke, F. Jelinek, and J. Raviv, "Optimal decoding of linear codes for minimizing symbol error rate (Corresp.)," *IEEE Trans. Inf. Theory*, vol. 20, no. 2, pp. 284–287, Mar. 1974.
- [13] S. ten Brink, "Designing iterative decoding schemes with the extrinsic information transfer chart," *AEU Int. J. Electron. Commun.*, vol. 54, no. 6, pp. 389–398, Nov. 2000.
- [14] S. Dolinar and D. Divsalar, "Weight distributions for turbo codes using random and nonrandom permutations," Jet Propulsion Lab., Pasadena, CA, USA, TDA Prog. Rep. 42-122, Apr./Jun. 1995, pp. 56–65.